Vacuum 215 (2023) 112302

Contents lists available at ScienceDirect

Vacuum

journal homepage: www.elsevier.com/locate/vacuum

Study of a low-energy collimated beam electron source and its application in a stable ionisation gauge

Zhuoya Ma [a], Detian Li [a,*], Huzhong Zhang [a,**], Peter Wurz [b], Rico Georgio Fausch [b], Yongjun Cheng [a], Peng Yao [a], Jinguo Ge [a], Xiaodong Han [a,c], Gang Li [a], Yongjun Wang [a], Changkun Dong [d]

[a] Science and Technology on Vacuum Technology and Physics Laboratory, Lanzhou Institute of Physics, Lanzhou, 73000, China
[b] Physics Institute, University of Bern, 3012, Bern, Switzerland
[c] School of Aerospace Engineering, Xiamen University, Fujian, 361102, China
[d] Institute of Micro-Nano Structures & Optoelectronics, Wenzhou University, Wenzhou, 325035, China

ARTICLE INFO

Keywords:
Electron source
Carbon nanotube
Ionisation vacuum gauge
Low-energy collimated beam

ABSTRACT

Stable ionisation vacuum gauges obtain stable sensitivity by controlling both the well-defined electron trajectory and electron energy in the ionisation volume. To achieve this goal, a collimated electron beam and large ionisation cross-section are required as the electrons enter the ionisation volume. In this paper, a low-energy electron source based on carbon nanotubes is designed to realise a collimated electron beam by the addition of specialised deceleration and focus electrodes. The experimental transmission is approximately 25%, which is in good agreement with the simulation results. Furthermore, a simulation study is carried out combining the electron source with the components of a novel stable ionisation gauge. The numerical simulation results show a sensitivity of 0.250 Pa^{-1}. It provides an important reference for the development of stable ionisation gauge based on the field emission cathode.

1. Introduction

Carbon nanotube (CNT) is an ideal electron source material with stable physical and chemical properties, high aspect ratio, small radius of curvature, and excellent electrical and thermal conductivity [1–3]. Electron sources made by CNT have advantages of small size, fast response and low power consumption. Such sources have been applied in various vacuum electronic devices such as X-ray tubes [4], travelling wave tubes [5,6] and electron guns [7,8]. In the past 20 years, many scholars have made attempts to replace hot filaments in ionisation gauges with CNT electron sources due to the high mechanical strength, robustness against thermal effects and excellent field emission characteristics in vacuum environment [9]. In 2004, Dong and Myneni [10] used a CNT electron source to replace the hot filament for the first time in an extractor gauge, achieving a sensitivity of 0.03 Pa^{-1} by suppressing the thermal effects of hot filament effectively, and the measurement errors were ±10% at 10^{-6} Pa. Knapp [11] studied CNT electron sources with hairy surface structures in Bayard-Alpert (B-A) gauges and the sensitivities changed from 0.10 to 0.15 Pa^{-1}. Liu et al. [12] designed a CNT electron source with a shielded electrode and applied it to B-A gauge, achieving the sensitivity of 0.05 Pa^{-1}. Li et al. [13,14] carried out research on the application of CNT electron sources in a B-A gauge and an extractor gauge, which improved the performance of the CNT cathode and obtained good measurement linearity from 10^{-8} Pa to 10^{-4} Pa.

Recently, Jousten, Jenninger and Bundaleski et al. [15–17] reported a novel ionisation gauge with a thermionic emission cathode, and the new design obtained predicted sensitivity and good stability, making the gauge suitable as a reference standard. The novel gauge has provided a practical and feasible scheme for the design of stable gauges. The CNT electron source is expected to be used in this kind of gauge to eliminate thermal radiation outgassing, thermal disturbance of the gas environment and electron kinetic energy interference [1,18], which would make the gauge more stable and reliable. However, replacing the hot filament directly by the CNT electron source in the conventional gauges would increase the energy of the electron in the ionisation volume to hundreds of electron volts and make the electron trajectories to be

* Corresponding author.
** Corresponding author.
E-mail addresses: lidetian@hotmail.com (D. Li), janehuge@126.com (H. Zhang).

https://doi.org/10.1016/j.vacuum.2023.112302
Received 5 December 2022; Received in revised form 12 June 2023; Accepted 13 June 2023
Available online 14 June 2023
0042-207X/

dispersed and unpredictable. The high kinetic energy and uncontrollable trajectories of electrons could induce variations of the sensitivity. Therefore, the study on the CNT electron source with controllable electron energy and trajectory is of considerable interest for the stable gauges. In addition, the CNT electron sources suffer from long-term current instability, which is an important factor why ionisation gauges based on field emission sources are still unavailable for commercial application [19]. However, we consider that they still have potential for application in stable ionisation gauges for the following main reasons. Firstly, some research to improve the long-term current stability of CNT cathodes continues, with some breakthroughs [20–22]. Moreover, the ionisation gauge in this study has nearly uniform electron trajectories and energy distributions in the ionisation volume, so that the effect of the number of electrons changing on the sensitivity stability can be significantly reduced, thus effectively reducing the effect of current decay. Furthermore, the easy replaceability of the cathode can further reduce the impact of this defect.

This paper shows the development of a new CNT electron source, which enables the introduction of a low-energy collimated electron beam with uniform and stable trajectories. Then, we combined the CNT electron source with the components of the novel gauge proposed by Jousten et al. [15]. The well-defined electrons trajectories in the gauge were simulated and the sensitivity was studied. This ionisation vacuum gauge aims for high stable sensitivity (with an annual uncertainty <1%) in the range of 10^{-2} Pa to 10^{-6} Pa.

2. Low-energy collimated beam electron source

2.1. Modelling and simulation

The structure of the designed electro-optical system based on the CNT electron source is shown in Fig. 1. The system includes a CNT electron source, an ionisation cage and an electron collector. The CNT electron source consists of a CNT cathode, a gate, a deceleration electrode and a focus electrode. The emission region of the CNT cathode defined in the simulation is a circular sheet with a diameter of 1.0 mm. The gate has square mesh with side length and wire diameter of 0.225 mm and 0.03 mm respectively. The total diameter of the gate is 1.2 mm. The deceleration electrode has the diameter of 1.2 mm and the thickness of 0.13 mm. The focus electrode is a conical hole with the entrance diameter, the exit diameter and thickness of 1.54 mm, 1.00 mm and 1.00 mm respectively. The three vacuum gaps between the cathode, the gate, the deceleration electrode and the focus electrode are 0.15 mm, 0.18 mm and 0.20 mm respectively. The ionisation cage is the region enclosed by a gas inlet grid, an ion extraction grid and an electron beam inlet and outlet. The electron beam inlet and outlet have the same shape with the diameter of 1.00 mm and the thickness of 0.58 mm. The electrons are extracted by the gate and subsequently collimated by the deceleration and focus electrodes. They then enter the ionisation cage and are collected by the electron collector.

We simulated the electron optical system with SIMION®, a software for ion and electro-optical simulations. 1000 initial electrons were randomly distributed on the surface of the CNT cathode. The emission energy was defined as 0.2 eV and the electron emission half-angle in the range of 0°–30°, respectively [23]. The voltages of the ionisation cage, the gate and the electron collector were respectively set to 0 V, 700 V and 10 V. We initially set the cathode voltage to −70 V, so that the electrons passing through the ionisation cage have an energy of approximately 70 eV according to the voltage difference between the CNT cathode and the ionisation cage. For most gas molecules, the electrons have a large ionisation cross section at such energies [24]. The ratio of electrons arriving in the ionisation cage to the total emitted electrons is defined as the electron transmission efficiency to evaluate the influence of deceleration and focus electrode voltage variations on the electron trajectories. The radial velocity v_r and axial velocity v_a of the electrons along the ionisation cage are applied to description the collimation of the electron beam.

In the simulation, we found that the high electron transmission efficiency and excellent collimation characteristics cannot be satisfied simultaneously. When both the deceleration voltage (U_d) and the focus voltage (U_f) were swept in the range of 0–1000 V, the maximum electron transmission efficiency reached 45.5% at $U_d = 1000$ V and $U_f = 280$ V, but the electrons were not well bunched and collimated as can be seen from Fig. 2(a). The electrons are accelerated before entering the focus electrode and the fluctuation range of v_r is 126.70 m/s to 4985.76 m/s with the mean value of 2609.03 m/s and the standard deviation of 1043.98 m/s, which can explain the divergence of the electron beam. Conversely, if the electrons are decelerated by the deceleration electrode before entering the focus electrode, v_r significantly decreases. As shown in Fig. 2(b), when $U_d = 0$ V and $U_f = 5$ V, the fluctuation range of v_r is 41.59 m/s to 1907.20 m/s, with the mean value of 650.07 m/s and the standard deviation of 432.83 m/s. The collimation of the electron beam is significantly improved. In summary, the setup of the deceleration electrode and focus electrode in this electron source effectively achieves low energy and collimation of the electron beam.

2.2. Experiment

The CNTs used in our experiments were directly grown on oxidation-reduction-treated stainless steel substrate with thermal chemical vapor deposition (CVD). It was produced at Wenzhou University, China. The same production process and detailed analysis was mentioned in our previous article [25]. As shown in Fig. 3(a), CNTs with a diameter of 1 mm were grown on a stainless steel substrate with a diameter of 1.5 mm. Fig. 3(b) shows the CNTs with an average diameter around 40 nm ~ 60 nm have homogeneous tubular structure.

Before the electron source tests, the CNTs were tested in a diode device test the variation of the emission current density under the uniform electric field. A molybdenum sheet was used as the electron collector and a ceramic sheet of 150 μm thickness was placed between the

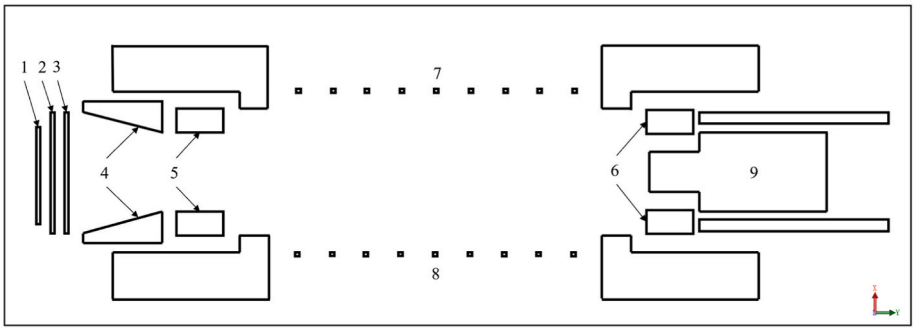

Fig. 1. Structural model, used for simulation of electro-optical system. 1-CNT cathode, 2-gate, 3-deceleration electrode, 4-focus electrode, 5-electron beam inlet, 6-electron beam outlet, 7-gas inlet grid, 8- ion extraction grid, 9-electron collector.

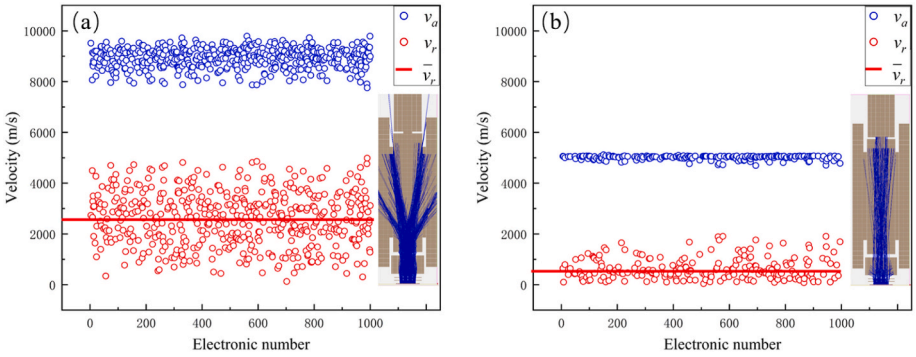

Fig. 2. Electron trajectories and velocity distributions. (a) $U_d = 1000$ V, $U_f = 280$ V. (b) $U_d = 0$ V, $U_f = 5$ V.

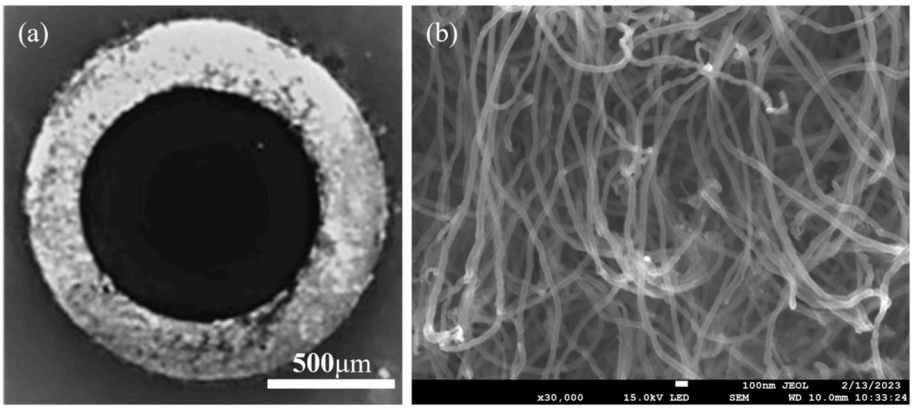

Fig. 3. (a) Optical photograph of CNT cathode. (b) The SEM image of the CNTs at 100 nm scale.

CNT and the Mo sheet. The tests were carried out at a pressure of 2×10^{-5} Pa. Fig. 4 shows the emission currents of the two tests have a good agreement. The macroscopic turn-on field for 10 μA/cm^2 is 2.2 V/μm, and an emitted current density of 13.2 mA/cm^2 was achieved when the field strength was increased to 5.8 V/μm.

According to the Fowler-Nordheim (F–N) theory [26], the field emission current density as a function of applied electric field can be expressed as

$$J = \frac{A}{\varphi}\beta^2 E^2 \exp^{-\frac{B\varphi^{3/2}}{\beta E}} \tag{1}$$

where J is the field emission current density in A/cm^2, A and B are expressed as the linear constant and exponential factor at room temperature, respectively, with $A = 1.54 \times 10^{-6}$ A V^{-2} eV, $B = 6.83 \times 10^7$ cm^{-1} V eV$^{-3/2}$. Φ is the work function of the emitter, $\Phi = 4.95$ eV for the typical multiwall CNT [27]. E is the CNT surface electric field strength, defined as the average electric field between the cathode and the extractor in V/cm. Since the tips of CNTs are sharp and have a higher charge density, there is a significant increase in the local electric filed in their vicinity. β is the field enhancement factor, which is defined as the ratio of the local electric field around the emitter tip to the macroscopic electric field.

By transforming Eq. (1) and taking the natural logarithm, it can be converted into the following linear equation:

$$In\left(\frac{J}{E^2}\right) = In\left(\frac{A\beta^2}{\varphi}\right) - \frac{B\varphi^{3/2}}{\beta}\frac{1}{E} \tag{2}$$

The field enhancement factor β is an important factor for electron-emitting materials and can be derived from the slope of the F–N plot:

$$\beta = -B\frac{\varphi^{3/2}}{slope} \tag{3}$$

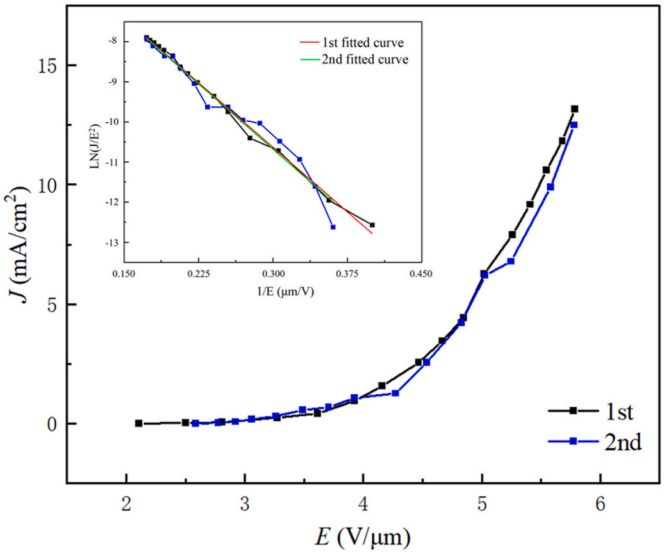

Fig. 4. Curve of emission current density as a function of applied electric field (J–E) and curve of Fowler-Nordheim (F–N) model of the CNT cathode in diode configuration.

Table 1
F–N curve fitting and calculated results.

Test number	Slope (V/cm)	Intercept	R^2	β
1st	−214824	1.335	0.995	3495
2nd	−217096	1.318	0.963	3465

This *slope* refers to the F–N fitted curve. The results shown in Table 1 were obtained by curve fitting of Eq. (2) to the data.

As shown in Fig. 5(a), a low-energy collimated beam CNT electron source was fabricated at University of Bern according to the experimental and simulation results above. The CNT arrays were mounted on the emitter holder and then assembled with the gate, the deceleration electrode and the focus electrode. The gate is a tungsten mesh with a wire diameter of 0.03 mm. Spacers made of ceramic are used to control the distance and isolate the electrodes. Fig. 5(b) shows the experimental setup for testing the electron source. The ionisation cage is a highly transparent cylindrical mesh structure with a constant electric field inside, and the electron collector is a circular sheet of 8 mm diameter to receive the electrons. In this case, the voltage of the decelerating and focus electrodes determine the trajectories and transmission efficiency of the electrons.

To suppress fluctuations of emission current, extend the lifetime of CNT films, and protect the DC power supply [21,28], a 1.24 MΩ ballast resistor was connected in series with the CNT cathode. A total of −175 V was applied to the CNT cathode and ballast resistor. The gate voltage was adjusted within the range of 0V–720V. The ionisation cage was grounded and a voltage of 10 V was applied to the electron collector. According to the emission current from the test, we can obtain the voltage division at the ballast resistor and the CNT cathode respectively.

As shown in Fig. 6(a), when U_d and U_f are fixed to 0 V and 5 V respectively, both the total emission current and the electron collector current increase as the voltage difference between the CNT cathode and gate increases. When the voltage difference between the CNT cathode and gate reaches 500V, electrons start to be received at the electron collector, and the operating temperature of the CNT electron source is 26 °C at this point. When the voltage difference reaches 780 V, the cathode emission current is 91.64 μA and the operating temperature of the electron source is 34 °C. The red curve in Fig. 6(a) corresponds to the black squares in Fig. 6(b). It can be seen that as the voltage difference increases, the emission current increases and the electron energy decreases due to the ballast resistor, during which the electron transmission efficiency gradually increases. When the voltage difference reaches the range of 722 V–780 V, corresponding to an electron energy of 123 eV–61 eV, the electron transmission efficiency reaches approximately 25% and stabilises. At this point, the voltage division at the CNT cathode varies in the range of −123 V to −61 V, and the −70 V settings in the simulations of Fig. 2 are also in this range. Further, a set of simulations was carried out in conjunction with the CNT cathode voltage division obtained experimentally, and the results are shown in Fig. 6(b) (red dots). It is observed that the simulated and experimental results are in good agreement over the electron energy range of 60–160 eV, and the main reason for the large difference in the range of 160–175 eV is the measurement error due to the very small current on the electron collector (as shown in Fig. 6(a)). This demonstrates that the introduction of the deceleration electrode and focus electrode allows for the bunching and collimation of electrons; the low electron energy can be controlled by adjusting the voltage difference between the CNT cathode and the ionisation cage. However, it should be noted that the simulation has two defects: (1) The absence of backscattered electron effects in the simulations leads to a high result. (2) The maximum resolution of 0.05 mm/grid that we can achieve does not accurately describe the shape of the gate mesh, where more electrons impact on the grid, resulting in a low result. These could also be the sources of discrepancies between simulation and experimental results.

3. Stable ionisation gauge based on low-energy collimated beam electron source

The low-energy collimated beam electron source is promising to be applied in the stable ionisation gauge. To study the performance of such new stable ionisation gauge, the optimised low-energy collimated electron source was combined with the components of the novel gauge reported by Jousten et al. [15,16], and a new model of stable ionisation gauge based on a CNT electron source was proposed, as shown in Fig. 7. According to the experiments, the gate voltage should be 700 V to ensure sufficient electrons to be successfully extracted. The electron collector is placed 47 mm far away from the inlet of ionisation cage. The voltages are set to 0 V at the CNT cathode, 250 V at the ionisation cage and 800 V at the electron collector. The voltages of the ion collector and the deflector are both 0 V. The cathode is a CNT array with a diameter of 1 mm. The field emission electron beam is extracted by the gate, introduced into the ionisation cage after passing through the deceleration and focus electrodes, and finally collected by the electron collector. In the process, the end of the electron beam trajectory is deflected by the deflector, which achieves the separation of the electron collection region and the ion collection region so that the X-ray photoelectrons cannot reach the ion collector. At the same time, the deflector can attract the ions desorbed from the surface of the electron collector and can push the secondary electrons back to the electron collector.

In SIMION simulation with cubic mesh, we simulated at 0.09 mm/grid, 0.08 mm/grid, 0.06 mm/grid, and 0.05 mm/grid resolutions and observed that the results converge below 0.08 mm/grid. Taking a resolution of 0.05 mm/grid for simulation, the number of grid units is 1.17×10^9 at this point. In order to visualise the effectiveness of the optimisation of the electron source, we simplified the electron collector to a flat disc to obtain the simulation results of the electron trajectories in Fig. 8(b) and Fig. 8(c). The CNT cathode is described as a flat plate emitter, and 1000 electrons randomly distributed on the surface of the CNT cathode during the simulation. We analysed the influence of deceleration and focus electrodes, as shown in Fig. 8(b). The electrons disperse rapidly after passing through the inlet frame when only the conventional CNT cathode and gate were assembled as electron source, resulting in an angular distribution of 0°–8° along the outgoing direction of the electron beam and an average radius distribution of 5.910 ± 0.029 mm as the electrons reach the electron collector. However, as shown in Fig. 8(a) and 8(c), the optimised structure of the low-energy collimated electron source was used, an average radius distribution was only 1.816 ± 0.023 mm with significantly less dispersion in the 47 mm path, and the electron beam angle distribution is 0°–2°. At this point, the voltages of deceleration and focus electrode are 500 V and

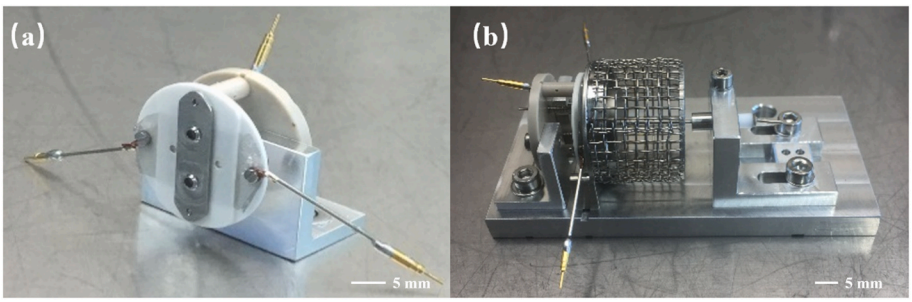

Fig. 5. (a) CNT electron source. (b) Experimental setup.

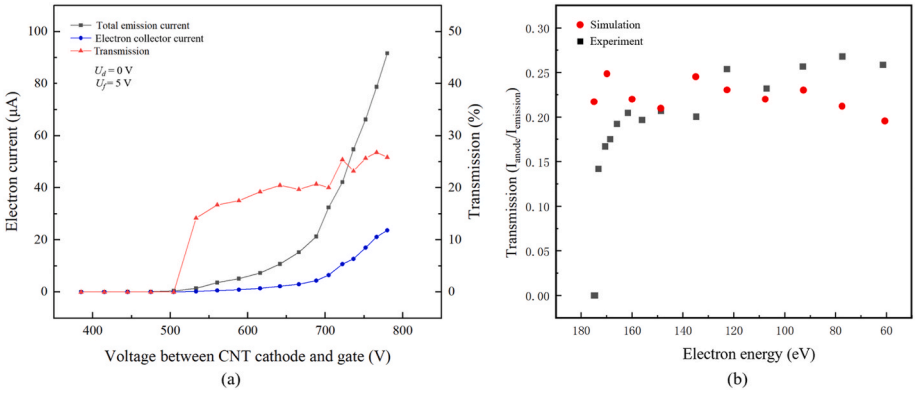

Fig. 6. Results of Electron Source experimental tests. (a) Variation of total emission current, electron collector current and transmission with the voltage difference between CNT cathode and gate. (b) Variation of transmission with electron energy in experiments and simulations.

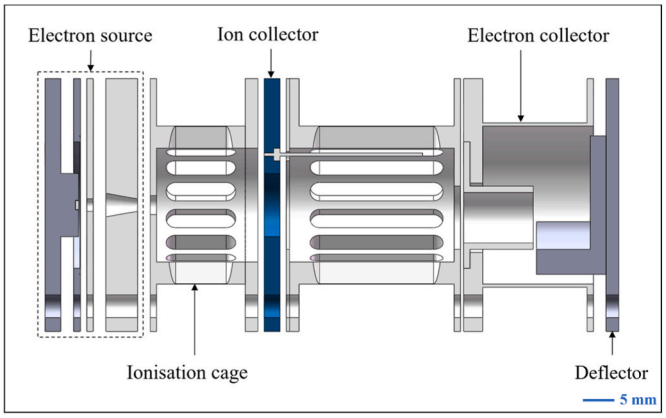

Fig. 7. Structure of prototype of stable ionisation gauge we are developing.

1000 V respectively. Thus, as depicted in Fig. 8(d), the electron paths in the stable ionisation gauge with low-energy collimated electron source have considerable collimation characteristics and the electrons are collected in beam by the electron collector after being deflected.

To analyse the energy consistency of electrons emitted from different sites in CNT array, 10 electrons are randomly distributed on the CNT cathode and electron energy is recorded along the entire Z-axis. Fig. 9(a) shows that the electrons have a stable energy distribution within the ionisation volume ($Z = 17.65$ mm to $Z = 64.65$ mm), where the electron energy reduction in the range 17.65 mm–35.9 mm is caused by the electric field at the grounding potential of the ion collector. The energy of electrons passing near the ion collector is in the range 65 eV–250 eV, which has a large collisional ionisation cross section for most gas molecules [24].

Ten simulations of the emission are carried out (1000 electrons randomly distributed on the CNT cathode). The electron transmission efficiency can be obtained by dividing the recorded number of electrons entering the ionisation cage by the number of emitted electrons, and the electron collection efficiency can be obtained by dividing the number of electrons reaching the electron collector by the number of electrons entering the ionisation cage. The results are shown in Fig. 9(b), the electron transmission efficiency is around 24% and the electron collection efficiency is 100%, which meets the design requirements of the well-defined electron trajectories and the stable electron energy distribution for a stable ionisation gauge.

According to the defining equation [29] of the sensitivity of the ionisation gauge, the mean sensitivity calculated by the discretization method [30]:

$$S = \frac{L\sigma}{kT} = \frac{\int \sigma(l)dl}{nkT} = \frac{\sum_i (\Delta l_i \cdot \sigma_i)}{nkT} \tag{4}$$

where n is the number of electrons entering the ionisation cage and L is the length of the effective electron trajectory. σ represents the ionisation cross section of an electron colliding with a gas molecule or atom. k is the Boltzmann constant and T is the temperature of background gas in the ionisation volume. The sensitivity for N_2 is 0.250 Pa^{-1} with a standard deviation of 7.67×10^{-5} Pa^{-1}. Jousten et al. reported 0.297 Pa^{-1} for the simulated sensitivity of the novel ionisation gauge, while 0.280 Pa^{-1} to 0.295 Pa^{-1} for the experimental sensitivity [15,16]. The simulation results of the both are in good agreement. The differences between the simulation results are mainly caused by variations in ionisation volume length, electron energies and the method of calculations for sensitivity simulations.

In addition, the influence of the following factors on the reliability of the simulation results was analysed:

1. Collision rebound of electrons on the electrodes.

The main reason for the 24% electron transmission efficiency in the simulation is that the actual transmission efficiency of the gate is only 30%. Therefore, only about 6% of the electrons will impact at the deceleration electrode and focus electrode. Meanwhile, due to the strong potential field between the focus electrode and the inlet of the ionisation cage and the conical hole structure of the focus electrode, only few of the electrons enter the ionisation region after the elastic collision bounce. As well, according to the principle of the gauge, the individual electrons entering the ionisation cage have nearly uniform $\Delta l \cdot \Delta\sigma$, so that small changes in the number of electrons will not significantly affect the sensitivity results.

2. Trajectory deviation due to collision of a few electrons with gas molecules.

This effect mainly affects the upper measurement limit of the gauge. A few electrons are deflected by collisions with gas molecules and thus not collected by the collector. Based on the maximum achievable electron collection efficiency $W = 1 - p \cdot S$ in the Reference [17], this effect is estimated to result in an upper measurement limit of approximately 10^{-2} Pa. The sensitivity calculation will be significantly affected when the pressure exceeds 10^{-2} Pa.

3. Secondary electrons produced on the electron collector and ion collector.

Due to the large potential difference of 800 V between the deflector

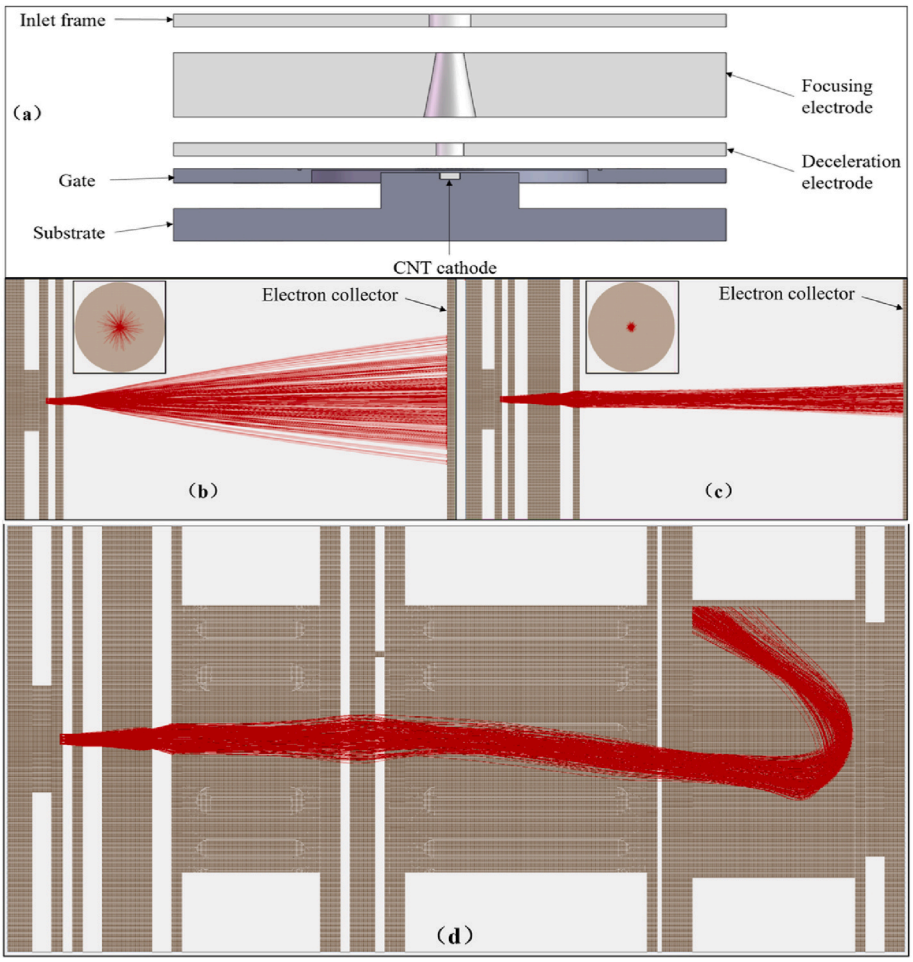

Fig. 8. (a) Structure of the electron source. (b) Electron trajectories before optimisation. (c) Electron trajectories after optimisation. (d) Electron trajectories throughout the gauge.

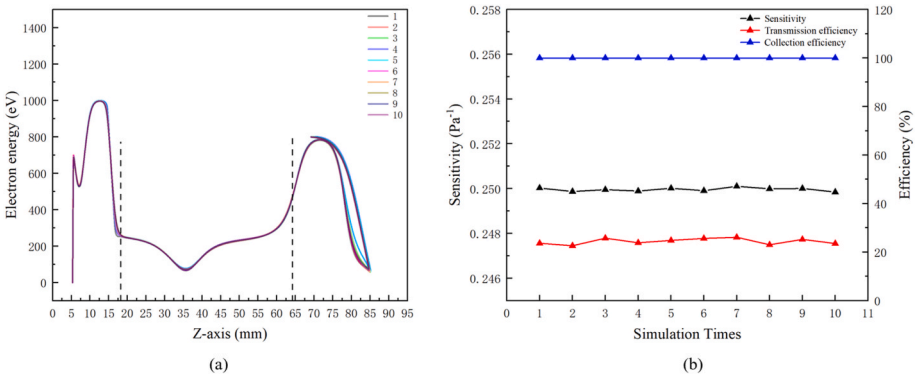

Fig. 9. Simulation results for stable ionisation gauge. (a) Energy consistency of ten electrons along Z-axis. (b) Calculation results of ten simulations.

and the electron collector and the shape of their respective structures, the escape probability of secondary electrons or backscattered electrons is very low.

However, the secondary electrons from the ion collector cannot be eliminated in this type of gauge. Therefore, the main focus to ensure the accuracy of the gauge is to stabilise its secondary electron yield induced by ions. It is noted that the formation of a uniform and sufficiently thick hydrocarbon layer on the electrode material could be expected to stabilise the secondary electron yield [31]. This process requires specific experiments to evaluate and fails to be quantified in the simulation.

4. ESD effect introduced by 24% electron transmission efficiency.

The ESD effect is the most significant influence on the lower measurement limit in the design of this structure and can have an adverse effect even greater than the thermal degassing and thermal radiation effects of the hot cathode. Besides the ESD effect at the electron collector, we note that about 70% of the electrons are lost in the process of inducing electrons by the gate, so we need to continue the research in two aspects: (a) Improve the electron transmission efficiency by optimising the gate structure. (b) Electrode material selection or material

coating to reduce the ESD effect.

4. Conclusion

In this paper, a low-energy collimated beam electron source based on the CNT cathode is designed. Simulations and experimental verification show that bunching and collimation of the electron beam can be achieved in this electron source using the deceleration and focus electrodes, and that the electron energy can be determined by the voltage difference between the CNT cathode and the ionisation cage. The electrode structure and voltage of this electron source were specifically optimised to meet the requirements of a stable ionisation gauge. The simulation results showed that the gauge realises a stable energy distribution of the electrons and well-defined electron trajectories in the ionisation volume. The theoretical sensitivity of the gauge is calculated to 0.250 Pa^{-1} with a standard deviation of 7.67 $\times$ 10^{-5} Pa^{-1}, providing an important reference for the development of a stable ionisation gauge based on CNT electron source.

In addition, the electron source has the advantages of simple structure and easy replacement. It can be applied to other types of ionisation gauges to eliminate defects of hot filament such as easy deformation, thermal radiation, thermal degassing and thermal evaporation. The CNT electron source provides a new research method for improving the sensitivity stability for ionisation gauges and for the measurement of high vacuum.

CRediT authorship contribution statement

Zhuoya Ma: Writing – review & editing, Writing – original draft, Software, Methodology, Investigation. **Detian Li:** Writing – review & editing, Supervision, Project administration. **Huzhong Zhang:** Writing – review & editing, Supervision, Project administration, Funding acquisition. **Peter Wurz:** Writing – review & editing, Funding acquisition. **Rico Georgio Fausch:** Writing – review & editing, Funding acquisition. **Yongjun Cheng:** Supervision. **Peng Yao:** Investigation. **Jinguo Ge:** Investigation. **Xiaodong Han:** Writing – review & editing. **Gang Li:** Writing – review & editing, Supervision. **Yongjun Wang:** Writing – review & editing. **Changkun Dong:** Supervision.

Declaration of competing interest

he authors declare that they have no known competing financial interests or personal relationships that could have appeared to influence the work reported in this paper.

Data availability

Data will be made available on request.

Acknowledgments

This work was supported in part by the National Natural Science Foundation of China (Grant No. 62171208) and base funding of the University of Bern.

References

[1] C. Edelmann, Field emitter-based vacuum sensors, Vacuum 86 (5) (2012) 556–571.
[2] H.S. Jang, H.-R. Lee, D.-H. Kim, Field emission properties of carbon nanotubes with different morphologies, Thin Solid Films 500 (1–2) (2006) 124–128.
[3] Y.-l. Zhang, L.-l. Zhang, P.-x. Hou, H. Jiang, L. Chang, H.-m. Cheng, Synthesis and field emission property of carbon nanotubes with sharp tips, N. Carbon Mater. 26 (1) (2011) 52–56.
[4] H. Sugie, M. Tanemura, V. Filip, K. Iwata, K. Takahashi, F. Okuyama, Carbon nanotubes as electron source in an x-ray tube, Appl. Phys. Lett. 78 (17) (2001) 2578–2580.
[5] H.J. Kim, J.J. Choi, J.-H. Han, J.H. Park, J.-B. Yoo, Design and field emission test of carbon nanotube pasted cathodes for traveling-wave tube applications, IEEE Trans. Electron. Dev. 53 (11) (2006) 2674–2680.
[6] J. Zhang, J. Xu, D. Ji, H. Xu, M. Sun, L. Wu, X. Li, Q. Wang, X. Zhang, Development of an electron gun based on CNT-cathode for traveling wave tube application, Vacuum 186 (2021), 110029.
[7] S.A. Getty, T.T. King, R.A. Bis, H.H. Jones, F. Herrero, B.A. Lynch, P. Roman, P. Mahaffy, Performance of a Carbon Nanotube Field Emission Electron Gun, Micro (MEMS) and Nanotechnologies for Defense and Security, SPIE, 2007, pp. 264–275.
[8] J. Lim, A.P. Gupta, S.J. Yeo, M. Kong, C.-G. Cho, S.H. Kim, J.S. Ahn, M. Mativenga, J. Ryu, Design and fabrication of CNT-based ${E} $-Gun using stripe-patterned alloy substrate for X-ray applications, IEEE Trans. Electron. Dev. 66 (12) (2019) 5301–5304.
[9] Y. Saito, S. Uemura, Field emission from carbon nanotubes and its application to electron sources, Carbon 38 (2) (2000) 169–182.
[10] C. Dong, G.R. Myneni, Carbon nanotube electron source based ionization vacuum gauge, Appl. Phys. Lett. 84 (26) (2004) 5443–5445.
[11] W. Knapp, D. Schleussner, M. Wüest, Investigation of ionization gauges with carbon nanotube (CNT) field-emitter cathodes, in: Journal of Physics: Conference Series, IOP Publishing, 2008, 092007.
[12] H. Liu, H. Nakahara, S. Uemura, Y. Saito, Ionization vacuum gauge with a carbon nanotube field electron emitter combined with a shield electrode, Vacuum 84 (5) (2009) 713–717.
[13] D. Li, Y. Cheng, Y. Wang, H. Zhang, C. Dong, D. Li, Improved field emission properties of carbon nanotubes grown on stainless steel substrate and its application in ionization gauge, Appl. Surf. Sci. 365 (2016) 10–18.
[14] D. Li, Y. Cheng, H. Zhang, Y. Wang, J. Sun, M. Dong, Investigation of an extractor gauge modified by carbon nanotubes emitter grown on stainless steel substrate, Vacuum 123 (2016) 69–75.
[15] B. Jenninger, J. Anderson, M. Bernien, N. Bundaleski, H. Dimitrova, M. Granovskij, C. Illgen, J. Setina, K. Jousten, P. Kucharski, C. Reinhardt, F. Scuderi, R.A.S. Silva, A. Stöltzel, O.M.N.D. Teodoro, B. Trzpil-Jurgielewicz, M. Wüest, Development of a design for an ionisation vacuum gauge suitable as a reference standard, Vacuum 183 (2021), 109884.
[16] K. Jousten, M. Bernien, F. Boineau, N. Bundaleski, C. Illgen, B. Jenninger, G. Jönsson, J. Šetina, O.M. Teodoro, M. Vičar, Electrons on a straight path: a novel ionisation vacuum gauge suitable as reference standard, Vacuum 189 (2021), 110239.
[17] N. Bundaleski, C. Adame, M. Bernien, C. Illgen, B. Jenninger, K. Jousten, F. Scuderi, R. Silva, A. Stöltzel, J. Šetina, Novel ionisation vacuum gauge suitable as a reference standard: influence of primary electron trajectories on the operation, Vacuum 201 (2022), 111041.
[18] T. Verbovšek, J. Šetina, Investigating the interactions of hydrogen and nitrogen with the tantalum cathode of a novel ionization vacuum gauge with a straight path of electrons, Measurement (2022), 111379.
[19] D. Li, Y. Wang, Y. Cheng, Y. Feng, L. Zhao, H. Zhang, J. Sun, C. Dong, An overview of ionization gauges with carbon nanotube cathodes, J. Phys. Appl. Phys. 48 (47) (2015), 473001.
[20] D. Leberl, R. Ummethala, A. Leonhardt, B. Hensel, S.F. Tedde, O. Schmidt, O. Hayden, Characterization of carbon nanotube field emitters in pulsed operation mode, J. Vac. Sci. Technol.B. Nanotechnol.Microelectron. : Mater.Process.Meas., Phenom. 31 (1) (2013), 012204.
[21] Y. Wang, D. Li, W. Sun, J. Sun, G. Li, H. Zhang, Z. Xi, X. Pei, Y. Li, Y. Cheng, Synthesis and field electron emission properties of multi-walled carbon nanotube films directly grown on catalytic stainless steel substrate, Vacuum 149 (2018) 195–199.
[22] H. Tang, R. Liu, W. Huang, W. Zhu, W. Qian, C. Dong, Field emission of multi-walled carbon nanotubes from pt-assisted chemical vapor deposition, Nanomaterials 12 (3) (2022) 575.
[23] S. Iacobucci, M. Fratini, A. Rizzo, Y. Zhang, M. Cole, W. Milne, S. Lagomarsino, A. Liscio, G. Stefani, Carbon nanotube—based cold cathodes: field emission angular properties and temporal stability, J. Appl. Phys. 120 (16) (2016), 164305.
[24] W. Hwang, Y.K. Kim, M.E. Rudd, New model for electron-impact ionization cross sections of molecules, J. Chem. Phys. 104 (8) (1996) 2956–2966.
[25] H. Zhang, D. Li, P. Wurz, A. Etter, Y. Cheng, C. Dong, W. Huang, Performance of a low energy ion source with carbon nanotube electron emitters under the influence of various operating gases, Nanomaterials 10 (2) (2020) 354.
[26] S. Parveen, A. Kumar, S. Husain, M. Husain, Fowler Nordheim theory of carbon nanotube based field emitters, Phys. B Condens. Matter 505 (2017) 1–8.
[27] M. Shiraishi, M. Ata, Work function of carbon nanotubes, Carbon 39 (12) (2001) 1913–1917.
[28] H. Suga, H. Abe, M. Tanaka, T. Shimizu, T. Ohno, Y. Nishioka, H. Tokumoto, Stable multiwalled carbon nanotube electron emitter operating in low vacuum, Surf. Interface Anal: Int. J.Devoted.Dev. Appl.Tech.Anal.Surfaces.Interfac. thin films 38 (12-13) (2006) 1763–1767.
[29] F. Nakao, Determination of the ionization gauge sensitivity using the relative ionization cross-section, Vacuum 25 (9–10) (1975) 431–435.
[30] W. Jianping, L. Detian, C. Yongjun, H. Yingjie, G. Jinguo, Y. Peng, Z. Huzhong, Sensitivity calculation of ionization gauge based on an accurate numerical method, Chin. J. Vac. Sci. Technol. 42 (2022) 170–177, 03.
[31] I. Figueiredo, N. Bundaleski, O. Teodoro, K. Jousten, C. Illgen, Influence of ion induced secondary electron emission on the stability of ionisation vacuum gauges, Vacuum 184 (2021), 109907.